Electronic Supplementary Material (ESI) for Dalton Transactions.
This journal is © The Royal Society of Chemistry 2020

Supporting Information

P-functionalized and O-deficient TiO_n/VO_m nanoparticles grown on Ni foam as electrode for supercapacitor: epitaxial grown heterojunction and visible-light-driven photoresponse

Keyu Tao, Lian Wang, Yang Hai and Yun Gong*

Department of Applied Chemistry, College of Chemistry and Chemical Engineering, Chongqing University, Chongqing 401331, P. R. China. E-mail: gongyun7211@cqu.edu.cn; Tel: +86-023-65678932

Table S1 The names of the samples synthesized under different conditions.

Sample	First-step hydrothermal synthesis		Second-step phosphorization	
	V_2O_5 (mg)	H_2O_2(mL)/H_2O(mL)	NaH_2PO_2 (mg)	$TiCl_4$ (μL)
VO_m/NF	20	2/8	/	/
P-VO_m/NF	20	2/8	100	/
P-TiO_n-VO_m/NF	20	2/8	100	50
P-TiO_2-VO_m/NF	20	2/8	100	150

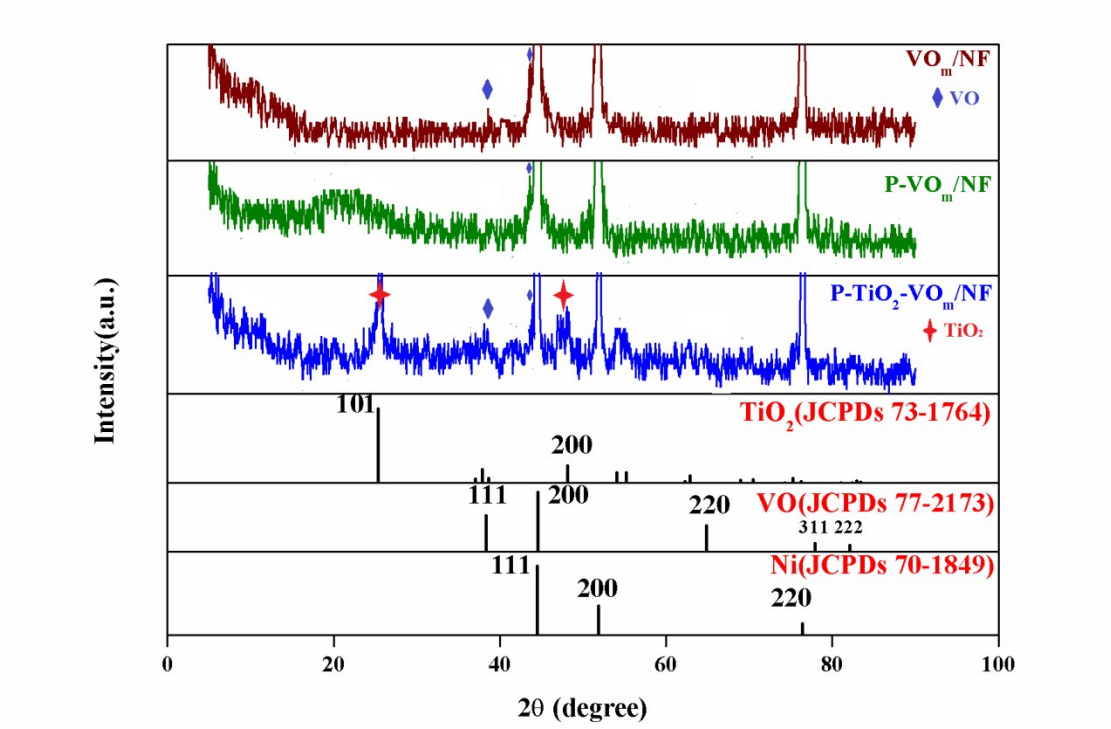

Fig. S1 XRD patterns of VO_m/NF, P-VO_m/NF, P-TiO_2-VO_m/NF and the standard

profiles.

Table S2 The atomic percentages (at. %) in the samples.

Sample	VO_m/NF	P-VO_m/NF	P-TiO_n-VO_m/NF		P-TiO_2-VO_m/NF
			Before cycling test	After cycling test	
Ni	71.8	11.1	14.4/11.8	25.7	5.6
V	14.6	9.1	32.9/9.8	0.6	1.0
O	13.6	50.4	42.1/65.4	63.1	66.6
P	/	29.4	9.1/8.4	9.1	3.6
Ti	/	/	1.5/4.6	0.6	23.2
K	/	/	/	0.9	

(a)

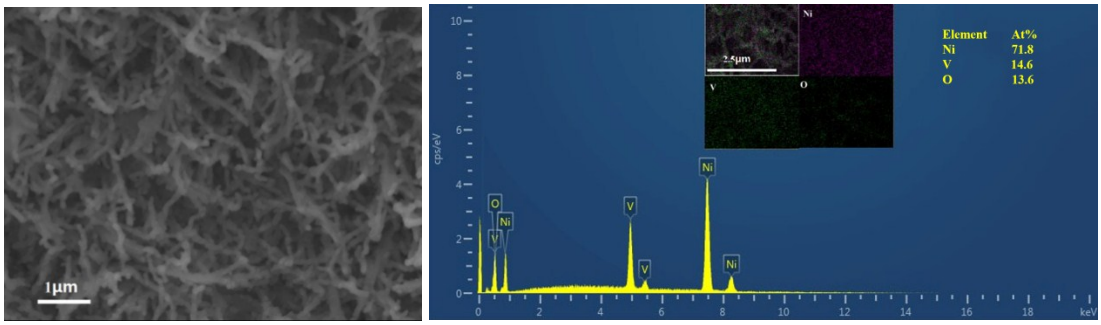

Fig. S2 SEM (**a**) and EDS (**b**) as well as elemental mappings (inset) of VO_m/NF.

(a) **(b)**

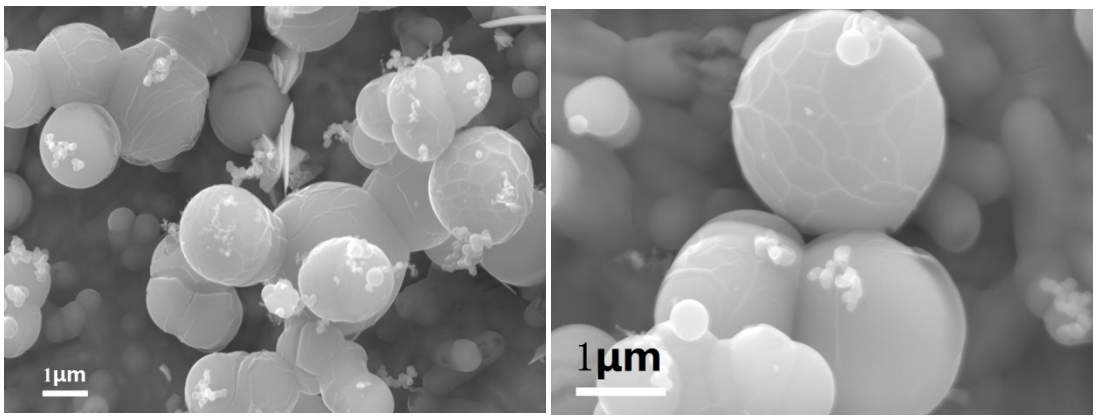

(c)

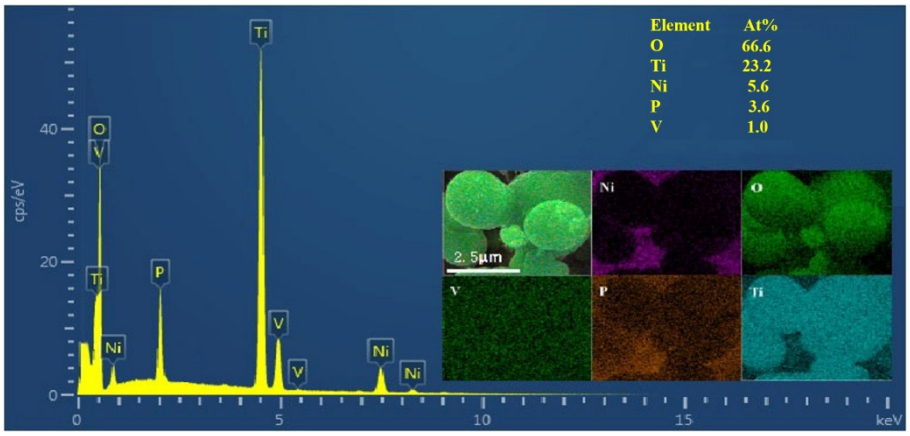

Fig. S3 SEM (**a, b**) and EDS as well as elemental mappings (inset) (**c**) of P-TiO_2-VO_m/NF.

Table S3 Comparison of XPS binding energies (eV) in VO_m/NF, P-VO_m/NF and P-TiO_n-VO_m/NF.

Sample		VO_m/NF	P-VO_m/NF	P-TiO_n-VO_m/NF
Ni 2p	Ni(0)	852.4	852.4	852.4
	Ni^{2+}	856.2/873.7	856.2/873.7	856.2/873.7
V 2p	V^{2+}	/	512.6	/
	V^{4+}	516.8	516.2/522.3	516.3
	V^{5+}	517.5/524.5	518.0/524.2	517.2/524.5
O 1s	Metal-O	530.4	531.1	531.3
	-OH	531.8	532.4	533.0
P 2p	Metal-P	/	129.0	133.6
	P-O	/	129.2	134.4
Ti 2p	Ti^{2+}	/	/	455.4/460.2
	Ti^{3+}	/	/	456.8/462.0
	Ti^{4+}	/	/	458.6/464.2

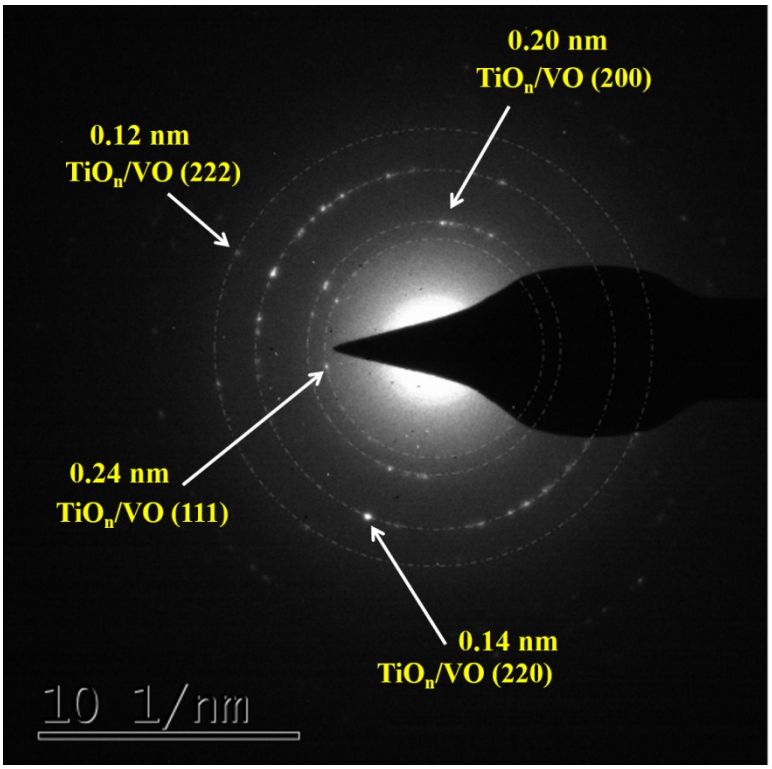

Fig. S4 SAED pattern of the nanoparticles in P-TiO_n-VO_m/NF.

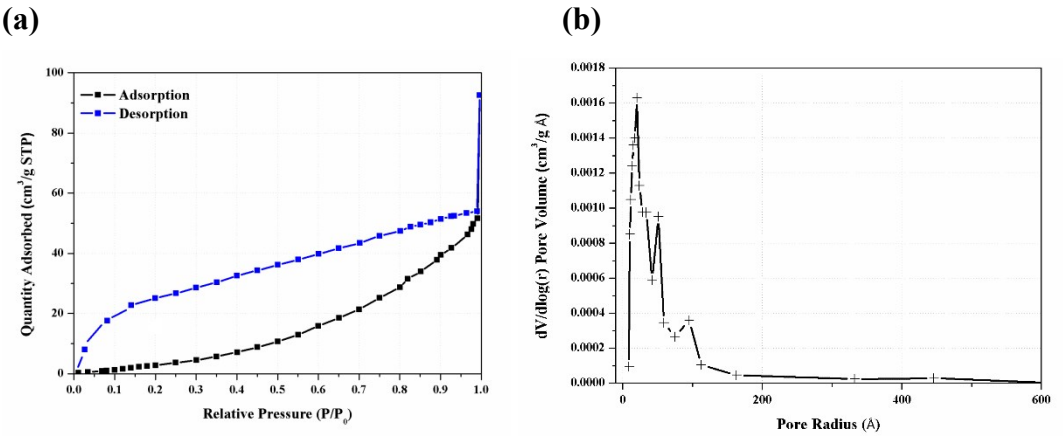

Fig. S5 Nitrogen adsorption/desorption isotherm curve (**a**) and pore size distribution curve (**b**) of P-TiO_n-VO_m/NF.

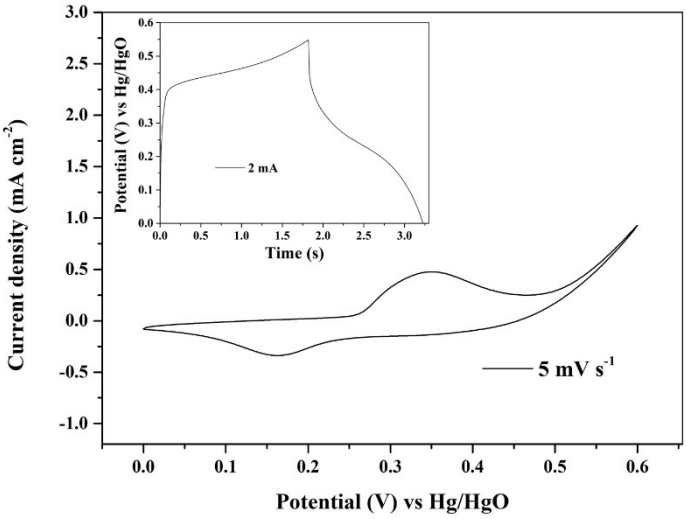

Fig. S6 The electrochemical performance of PH_3 treated bare NF.

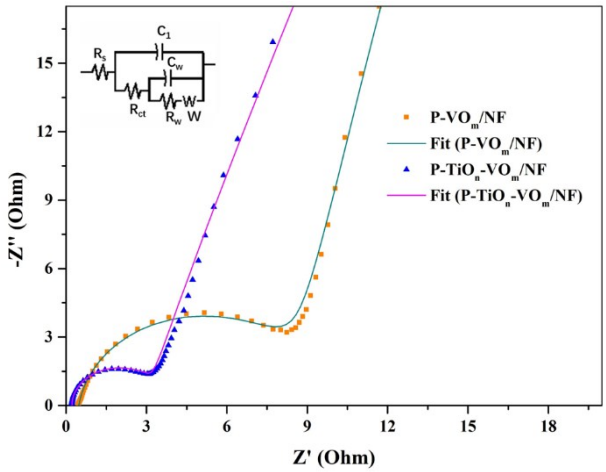

Fig. S7 The EIS plots of P-VO_m/NF and P-TiO_n-VO_m/NF.

(a) **(b)**

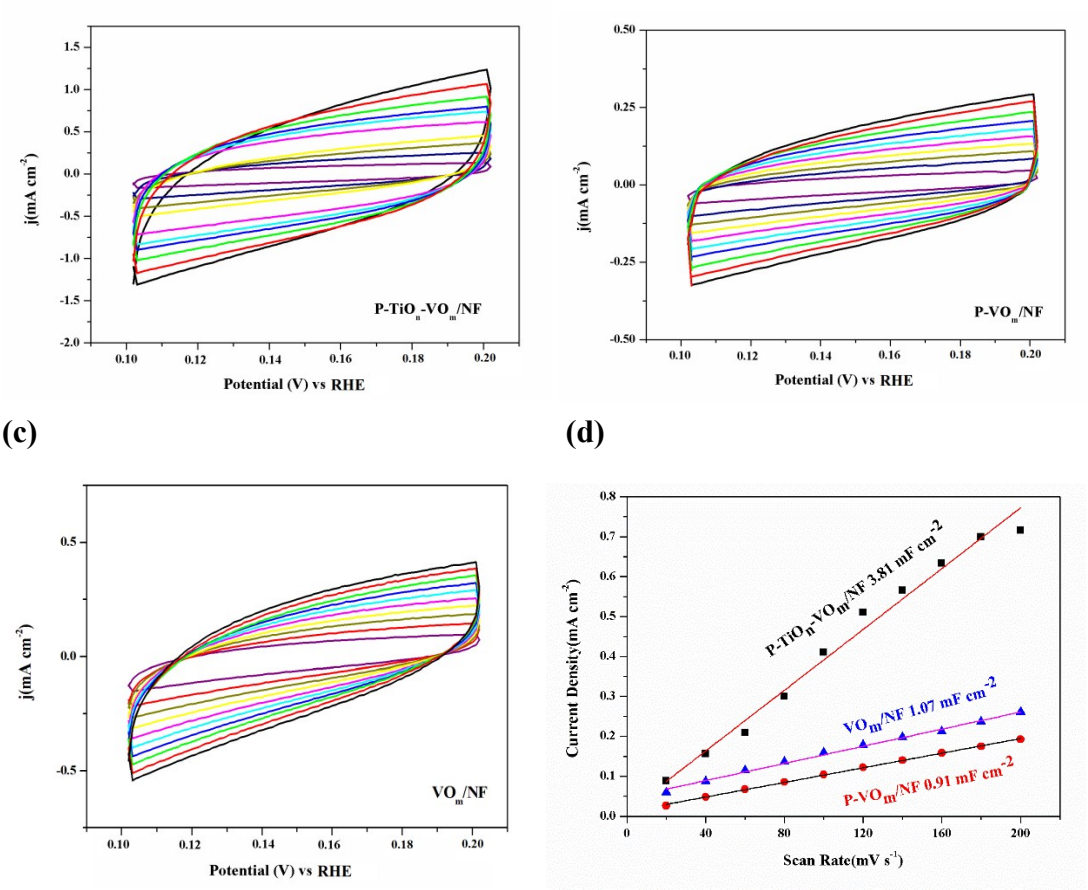

Fig. S8 CV curves (20-200 mV s^{-1}) at different scanning rates of P-TiO_n-VO_m/NF (**a**), P-VO_m/NF (**b**) and VO_m/NF (**c**). The relationship between capacitive currents at 0.15 V vs RHE and scanning rates (**d**).

Table S4 Comparison of electrochemical performances of previous titanium oxides and vanadium oxides reported previously.

Active material	Specific capacity	Electro-lyte	Super-capacitor	Energy density/Power density	Capacity retention	Ref.
OD-TiO_2/G	402 F g^{-1}	1 M KOH	OD-TiO_2/G//OD-TiO_2/G	14.1 Wh kg^{-1}/8.5 kW kg^{-1}	/	1
VO_x@MoO_3	683 F g^{-1}	5 M KCl	VO_x@MoO_3//MnO_2	1.63 mWh cm^{-3}/0.0325 W cm^{-3}	87 % (9000 cycles)	2
VO_2/AEG	78 mAh g^{-1}	4 M KOH	VO_2/AEG//C-V_2NO	41.6 Wh kg^{-1}/904 W kg^{-1}	93 % (10000 cycles)	3
GF+VO_2/HMB	485 F g^{-1}	1 M K_2SO_4	GF+VO_2/HMB//AC	14.5 Wh kg^{-1}/0.72 kW kg^{-1}	N/A	4
Co_3O_4/$Co_3(VO_4)_2$	847 F g^{-1}	2 M KOH	Co_3O_4/$Co_3(VO_4)_2$ //AC	38 Wh kg^{-1}/275 W kg^{-1}	95 % (5000 cycles)	5

HPCF@VN	241 F g^{-1}	6 M KOH	HPCF@VN// $Ni(OH)_2$	39.3 Wh kg^{-1}/400 W kg^{-1}	78 % (10000 cycles)	6
$VO(OH)_2$/ CNT	512 C g^{-1}	1 M $LiClO_4$	$VO(OH)_2$/ CNT// $VO(OH)_2$/ CNT	32.1 Wh kg^{-1}/63.7 W kg^{-1}	90 % (2000 cycles)	7
NiV_2S_4	639 C g^{-1}	6 M KOH	$Ni_3(VO_4)_2$// AC	45.1 Wh kg^{-1}/240 W kg^{-1}	91 % (2000 cycles)	8
P-TiO_n-VO_m/NF	785 C g^{-1}	2 M KOH	P-TiOn-VOm/NF//AC	37.2 Wh kg^{-1}/1 kW kg^{-1}	80 % (10000 cycles)	**This work**

Table S5 Parameters in the equivalent circuits for P-TiO_n-VO_m/NF at different stages.

	R_S /Ω cm^{-2}	C_1 /F cm^{-2}	R_{ct} /Ω cm^{-2}	W /Ω cm^{-2}	R_w /Ω cm^{-2}	C_w /F cm^{-2}
Initial	0.12	3.0×10^{-4}	1.86	0.008	0.01	1.2×10^{-4}
After 10000 cycles	0.23	3.4×10^{-4}	13.43	0.009	0.01	2.3×10^{-4}
Under illumination	1.33	4×10^{-4}	1.39	0.007	0.01	0.001

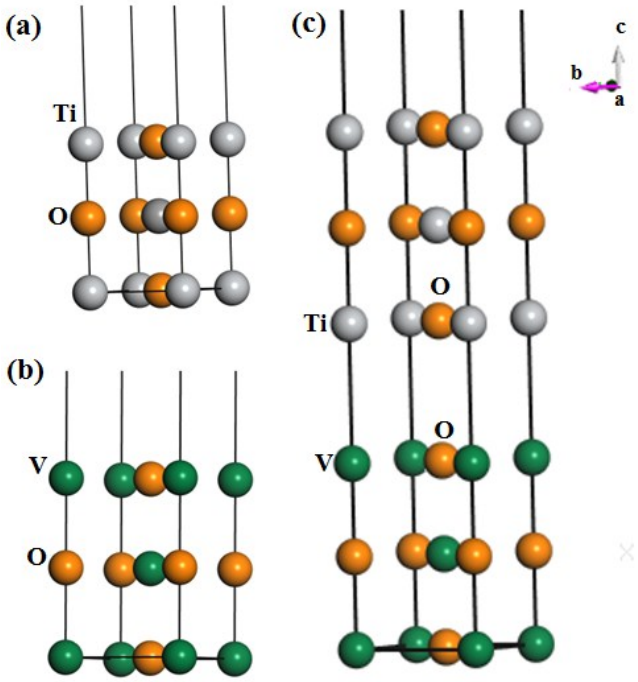

Fig. S9 Crystal structures of $(TiO_{1.250})_{3.07}$ (**a**), VO (**b**) and $(TiO_{1.250})_{3.07}$ /VO (**c**). Color codes: grey, Ti; orange, O; olive, V.

(a)

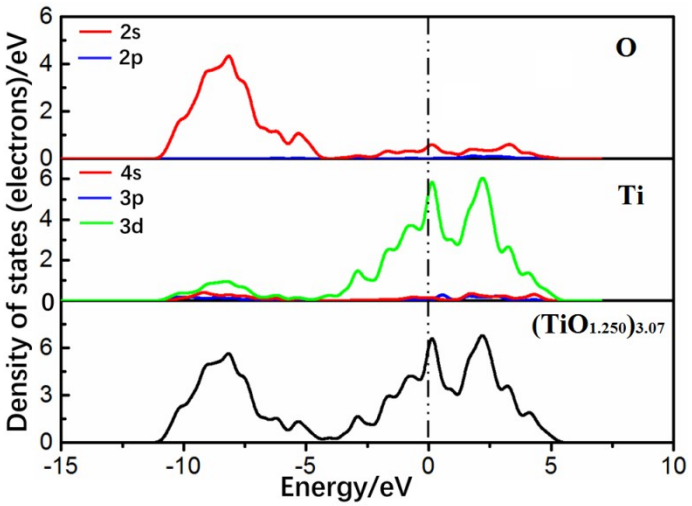
2s
2p
O
4s
3p
3d
Ti
(TiO1.250)3.07
Density of states (electrons)/eV
Energy/eV

(b)

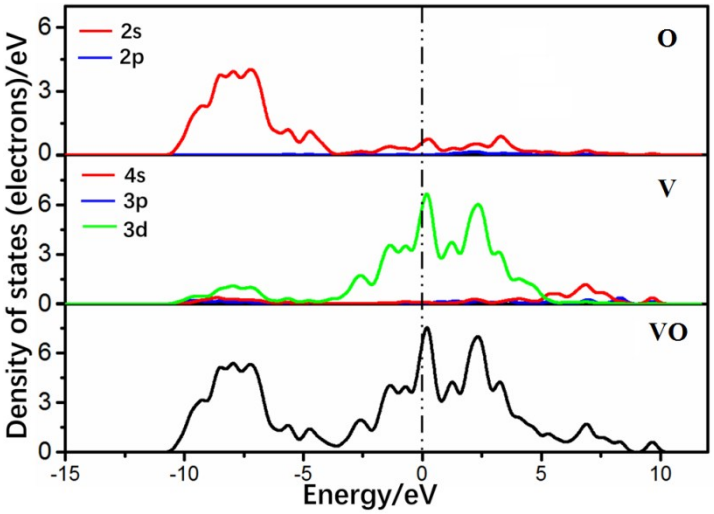
2s
2p
O
4s
3p
3d
V
VO
Density of states (electrons)/eV
Energy/eV

(c)

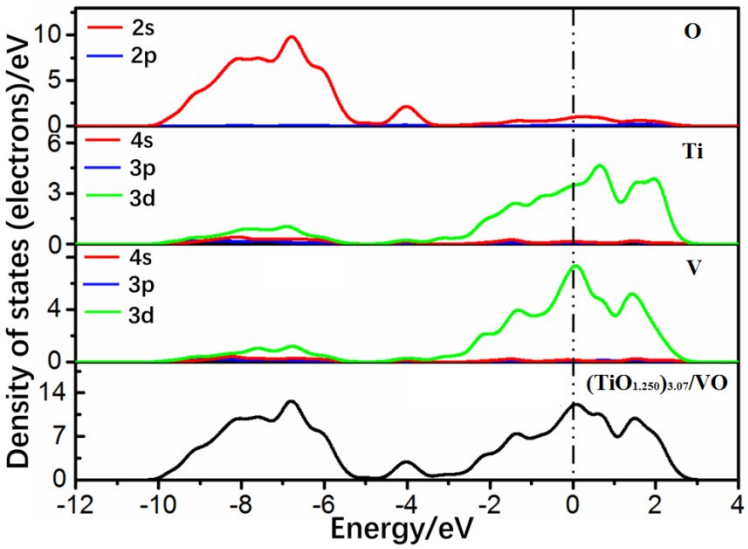
2s
2p
O
4s
3p
3d
Ti
4s
3p
3d
V
(TiO1.250)3.07/VO
Density of states (electrons)/eV
Energy/eV

Fig. S10 TDOS and PDOS of $(TiO_{1.250})_{3.07}$ (**a**), VO (**b**) and $(TiO_{1.250})_{3.07}$ /VO (**c**). Fermi level is denoted in dotted line. In the PDOS, blue, red and green lines represent s, p and d orbits, respectively.

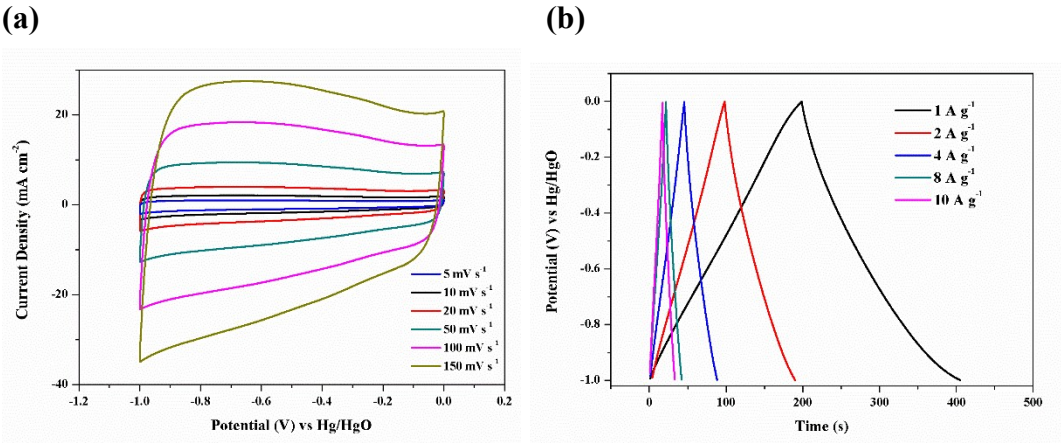

Fig. S11 The electrochemical performance of activated carbon (AC) electrode: CV curves at different scanning rates (**a**) and GCD curves at different current densities (**b**).

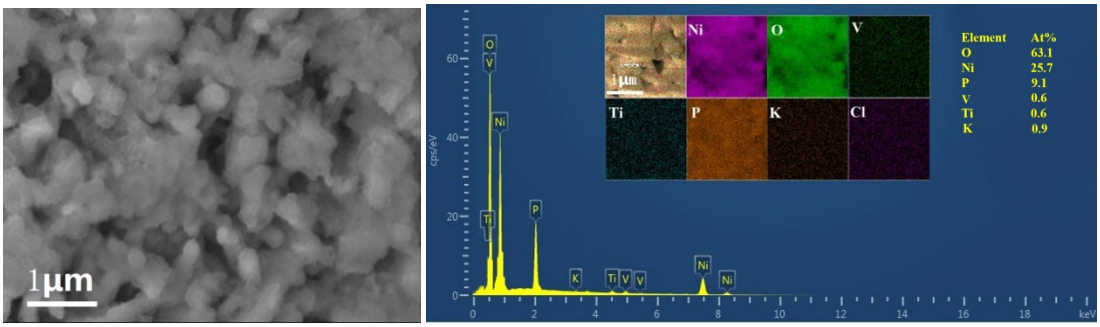

Fig. S12 SEM (**a**) and EDS (**b**) as well as elemental mappings (inset) of P-TiO_n-VO_m/NF after 10000 GCD cycles

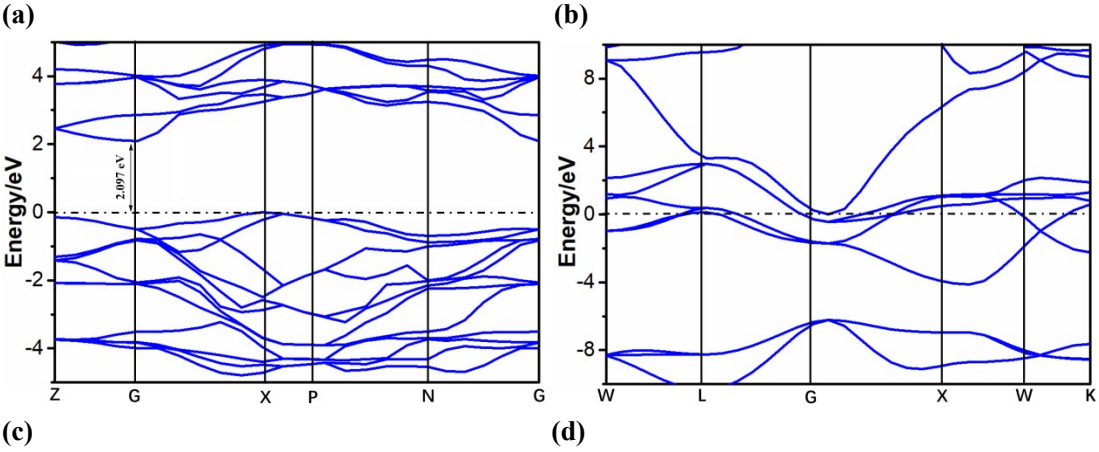

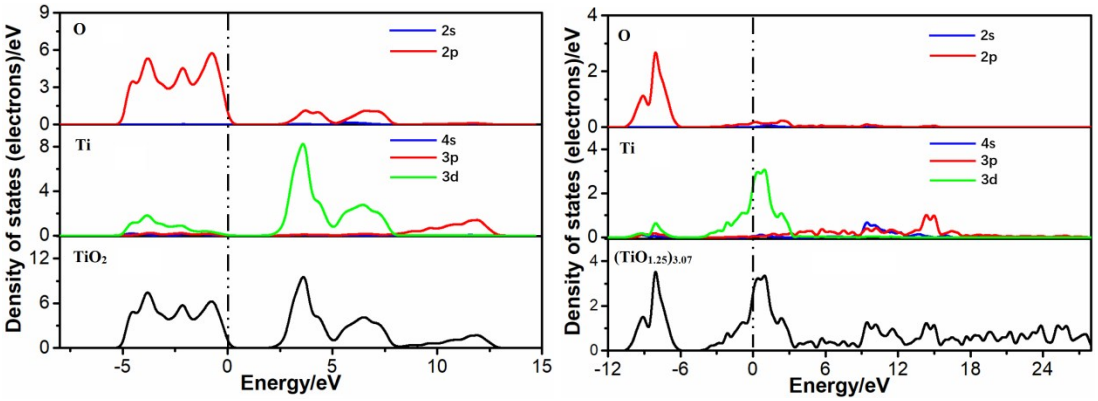

Fig. S13 Band structures (**a, b**) and TDOS as well as PDOS (**c, d**) for the anatase-type TiO_2 (**a, c**) and $(TiO_{1.25})_{3.07}$ (**b, d**). Fermi level is denoted in dotted line. In the PDOS, blue, red and green lines represent s, p and d orbits, respectively.

References:

1. S. Yang, Y. Li, J. Sun and B. Cao, *Journal of Power Sources*, 2019, **431**, 220-225.
2. S. Q. Wang, X. Cai, Y. Song, X. Sun and X. X. Liu, *Advanced Functional Materials*, 2018, **28**, 1803901.
3. N. M. Ndiaye, N. F. Sylla, B. D. Ngom, F. Barzegar, D. Momodu and N. Manyala, *Electrochimica Acta*, 2019, **316**, 19-32.
4. X. Xia, D. Chao, C. F. Ng, J. Lin, Z. Fan, H. Zhang, Z. X. Shen and H. J. Fan, *Materials Horizons*, 2015, **2**, 237-244.
5. W.B. Zhang, L.B. Kong, X.J. Ma, Y.C. Luo and L. Kang, *Journal of Power Sources*, 2014, **269**, 61-68.
6. F. Ran, Y. Wu, M. Jiang, Y. Tan, Y. Liu, L. Kong, L. Kang and S. Chen, *Dalton Transactions*, 2018, **47**, 4128-4138.
7. M. Chen, Y. Zhang, Y. Liu, J. Zheng and C. Meng, *Applied Surface Science*, 2019, **492**, 746-755.
8. R. Kumar, P. Rai and A. Sharma, *Journal of Materials Chemistry A*, 2016, **4**, 17512-17520.